Cummings T, Adamson R, Sugden A, Willis MJ.

Retrospective and predictive optimal scheduling of nitrogen liquefier units and the effect of renewable generation.

***Applied Energy* 2017,**

https://doi.org/10.1016/j.apenergy.2017.10.055

Retrospective and predictive optimal scheduling of nitrogen liquefier units and the effect of renewable generation

Thomas Cummings[a], Richard Adamson[a,b], Andrew Sugden[b] and Mark J. Willis[a]
[a]School of Chemical Engineering and Advanced Materials, Newcastle University, Newcastle upon Tyne, NE1 7RU, United Kingdom
[b]BOC Gases Ltd., Bawtry Road, Brinsworth, Rotherham, S60 5NT, United Kingdom
richard.adamson@boc.com, mark.willis@newcastle.ac.uk

Abstract

The construction and application of a multiple nitrogen liquefier unit (NLU) optimal scheduling tool is discussed. Constrained by customer demands and subject to electricity spot market prices over a week-ahead horizon, a retrospective optimiser (RO) determines the minimum scheduling costs. Plant start-up penalties and inter-site optimisation capabilities are incorporated into the optimisation model to emulate realistic operational flexibilities and costs. Using operational data, actual process schedules are compared to the RO results leading to improved process scheduling insights; such as increasing afternoon NLU operation during the spring to utilise lower power pricing caused by high solar generation. The RO is used to output a trackable load management key performance indicator to quantify potential and achieved scheduling improvements. Subsequently, correlations between renewable energy generation and spot market power prices are developed. Forecast pricing is used within a predictive optimiser (PO) to automatically generate an optimal schedule for the week ahead to meet projected customer demands. The RO provides potential hindsight savings of around 11%, and the PO up to 8% (representing significant cost savings for such energy intensive processes).

Keywords: production scheduling, retrospective optimisation, renewable generation, price forecasting, predictive optimisation, binary programming.

Highlights

- Development of a binary program to optimally schedule flexible power loads.
- Retrospective optimisation to generate a scheduling key performance indicator.
- Discovery of renewable generation and spot market correlations for early 2017.
- Predictive optimisation of power loads using power pricing forecasts.

Nomenclature

Abbreviations

ADRL – autoregressive distributed lag
ARIMA – autoregressive integrated moving average
ASU/s – air separation unit/s
DSM – demand side management
KPI/s – key performance indicator/s
LMP – load management plan
LN – liquid nitrogen
MILP – mixed integer linear programming
NLU/s – nitrogen liquefier unit/s
NW – network wide
OS – optimiser score
PO – predictive optimiser
RO – retrospective optimiser
RTP – real time pricing
TOU – time of use

Parameters

β	– optimiser score (MWh)	C_{MW}	– spot power cost (£/MWh)
Δ	– variation from average (generation, price)	G	– renewable penetration (%)
I_p	– inter-site optimisation penalty (£)	J	– cost function (£)
N	– number of (time periods or NLUs)	NW_{sav}	– network-wide savings (%)
R^2	– coefficient of determination (%)	P	– power demand (MWh)
μ	– average		
Variables			
δ	– start-up binary coefficient	w	– binary NLU running coefficient
z	– start-up coefficient		
Subscript/Superscripts			
A	– actual NLU operation	ab	– abortive start-up cost
int	– inter-site optimisation	j	– NLU number
NW	– network wide	p	– start-up power penalty
ren	– renewable generation source	$solar$	– solar generation
t	– discrete time point	$wind$	– wind generation
*	– optimal	^	– model

1.0 Introduction

Cryogenic air separation and the subsequent liquefaction of gaseous products is highly energy intensive, with process optimisation and optimal scheduling of power loads critical to minimise costs, see Adamson et al. (2017b). Where power loads are flexible, Merkert et al. (2015) describe demand side management (DSM) strategies which reallocate power usage from a period of peak power price to another at a lower off-peak price to reduce overall costs. Load scheduling strategies can be adopted by companies to lower costs whilst maintaining the same production volumes rather than carrying out temporary energy reduction activities detrimental to production. Most DSM activities introduce process inefficiencies, such as additional process starts and stops, but can minimise overall costs by avoiding peak power pricing consumption.

Driven by financial motivations alone, many studies have been conducted to research optimal scheduling practises for air separation processes. Daryanian et al. (1989) design an optimal operation scheduler for a week-ahead horizon with two key assumptions; (a) that hourly spot electricity prices are known, and (b) no additional energy costs are associated with start-up transitional modes. They compare the results to uniform plant scheduling with average spot pricing, revealing that varying production rate yields economic benefits. Similarly, Ierapetritou et al. (2002) determine an optimal schedule for air separation processes in real-time pricing (RTP) environments, improving flexibility by considering pricing changes using a mixed integer linear programming (MILP) model implemented within a commercially available solver. By assuming electricity prices are known for the initial periods (days) of a time horizon, an autoregressive integrated moving average (ARIMA) model can be developed to forecast prices for subsequent periods, assuming pricing can be explained by past values and the modelling error. Despite a maximum forecast accuracy of around 70%, simulation studies demonstrate that the forecasts were still effective at producing a near-optimal operating schedule due to following the pricing trends qualitatively rather than exactly quantitively. Karwan and Keblis (2007) deploy a similar rolling time horizon model to Ierapetritou et al.

(2002) concurring that unless plant utilisation is very high, optimal scheduling in a RTP environment often provides economic benefits. By participating in additional demand side response and grid run energy market schemes, scheme incentives can be added as cost savings to further boost the distribution network profits of optimal scheduling, Zhang et al. (2016).

Mitra et al. (2012a) generalise previous RTP optimal scheduling approaches by creating a deterministic discrete-time MILP model that allows optimal production planning whilst incorporating transitional plant models. Discrete-time formulations may not be fully representative of actual process dynamics (the solution inevitably approximates the real optimal schedule), but MILP approaches are easy to solve with allocation of resource units to tasks and the costs calculated linearly, Floudas and Lin (2005). Applied to an air separation unit (ASU) simulation using a commercial solver, the results estimated cost savings between 3.76% to 13.78% with the largest savings at lower plant utilisations. Model robustness is improved for suitability in situations where spot electricity prices are uncertain, see Mitra et al. (2012b), by deploying a historical pricing correlation to modify an uncertainty set, as proposed by Duzgun and Thiele (2010). Zhu et al. (2011) argue that the multiple scenario approach adopted by Karwan and Keblis (2007) and Ierapetritou et al. (2002) generates results that are too conservative to be deemed optimal, as customer demands must be met over all scenarios. Instead, they develop a non-linear model using probabilistic constraints, where simulation case-studies trade-off profit maximisation whilst considering a tangible customer satisfaction index.

Most articles in literature consider optimisation of whole air separation processes leading to the use of thousands of variables and constraints, and the requirement for commercial solvers on dedicated processors. In previous work, see Adamson et al. (2017a) and Adamson et al. (2017b), we develop strategies to model and minimise power consumption of a network of ASUs and compressors in real-time primarily to meet customer demand requirements using minimal computational requirements. In this paper, we propose a higher-level optimal scheduling approach which enables ideal DSM of external nitrogen liquefier units (NLUs) supplied by pure gaseous nitrogen from ASUs. Firstly, we design a retrospective optimiser (RO) to combine industrial operational data with grid generation data and spot market power pricing to retrospectively analyse current DSM technique effectiveness. Then, we develop a novel predictive optimiser (PO) using power pricing forecasts generated from correlations between renewable generation data and spot market power pricing. The RO and PO tools are developed using free to use and accessible software, enabling operators to track and improve load management of large power loads for cost reductions. As opposed to previous work, we consider the required running hours, time of use (TOU), start-up transitional mode costs and inter-site transfers of liquid product to deliver a true estimate of the potential DSM savings.

Retrospective analysis has been undertaken extensively in fields such as medicine, aviation and professional sports, see Croos-Dabrera et al. (2004), Dambier and Hinkelbein (2006) and Lewis et al. (2015). This approach has been proved effective in preventing aviation disasters, where black box analysis and learning has created an exceptional safety record, see Syed (2016). However, retrospective learning techniques are not typically utilised by the operational aspects of the process industries. By applying retrospective analysis techniques to the results obtained from the RO, it is demonstrated that a better understanding of optimal scheduling can be

developed to enable less conservative scheduling. The RO results are compared to the actual NLU schedule in hindsight to produce a DSM key performance indicator (KPI) for process scheduling. Retrospective analysis is carried out to compare the RO results to factors known to effect power pricing such as the time of day or increasing influence of renewable generation.

The increasing penetration of unpredictable and intermittent renewables, such as wind and solar PV, has led to renewable generation recently becoming the main cause of variation in power prices above the TOU, Merkert et al. (2015). The extreme difficulty associated with forecasting spot market electricity prices is well documented, see Zareipour et al. (2010). Methods proposed include regression modelling, Karakatsani and Bunn (2004), time-series modelling, Weron and Misiorek (2005) and statistical modelling, Guthrie and Videbeck (2007). Few modelling techniques investigate the market costs, that is the varying of price by traders' subject to the expected supply and demand at any given half-hour, with price primarily a function of reserve margin volume, Boogert and Dupont (2008). Margins are difficult to predict due to uncertainty of power station availability, demand and trader behaviour. However, these factors vary largely due to the TOU and weather conditions (temperature, wind strength and expected sunshine coverage) and can be roughly modelled using ARIMA data correlations.

An alternative to ARIMA modelling is deploying an autoregressive distributed lag (ARDL) approach. Hamid and Shabri (2017) use ARDL modelling to forecast palm oil pricing over a period of 15 years. ARDL dynamic models link the dependent variable to the lagged value of itself and its explanatory variables, whilst requiring the time series data to be stationary. However, Bentzen and Engsted (2001) discover that even with non-stationary data such as Denmark's domestic power consumption over a longer period of thirty-six years, ARDL models can be effective, albeit being much more complicated to deploy. Unfortunately, electricity pricing is typically short-term non-stationary due to repeating seasonal and weather effects, changing over days and weeks rather than years, affecting RTP immediately.

Swinand and Godel (2012) and Hall et al. (2015) describe how increased wind generation leads to a decrease in power prices, however the overall impact also includes the non-commodity cost increase to secure additional wind generation capacity. In addition, the embedded nature of small-scale wind and solar PV generation installations leads to poor visibility and trouble modelling actual renewable generation, National Grid (2016). The effect of renewable capacity on power prices is presented by Ofgem (2015), which highlights how strong intermittent generation can drive wholesale energy prices negative during low demand periods due to curtailment of wind generation. Therefore, a novel focus of this study is to consider and model how renewable penetration, defined as the percentage contribution of renewable generation to total electricity generation at a given time, can influence spot market power price, and be consequently used to forward optimally schedule of energy intensive process power loads. In this work, retrospective analysis discovers pricing trends to project the effect of predicted renewable generation. The RO and PO results, which are separated seasonally, show variation in the effectiveness of optimal scheduling techniques. This approach has been deployed previously in the medical sector to improve elective surgery scheduling, where RO results are compared to various factors prior to observing patient data trends, predicting factors forward and subsequently allowing a PO to schedule resources, Kargar et al. (2013).

1.1 Nitrogen liquefier units

External nitrogen liquefier units (NLUs) are large components of ASU plants and use significant amounts of power, around 10 megawatts (MW) per hour, to liquefy product nitrogen gas (often produced in excess by ASUs) and store it for gas network back-up and bulk liquid customers supplied by road tanker. Storage tank liquid levels are maintained between minimum contingency, for supply scheme and bulk demand back up in case of ASU failure, and the maximum capacity based on tank level alarm limits. NLUs consist of five key components: compressors, expansion turbines, heat exchangers, separators and an expansion valve. Nitrogen gas at low pressure enters the compressor suction, is discharged at high pressure and is split into two streams; one which is expanded and cooled through a turbine and recycled to the compressor inlet via a heat exchanger, and the other which passes through the heat exchanger and an expansion valve to generate cryogenic temperatures. The cryogenically cooled liquid stream passes through several separator stages at consecutively lower temperatures and pressures for bulk storage and flash gas is recycled to the compression stages. Figure 1 provides a schematic diagram of the liquefaction process and equipment.

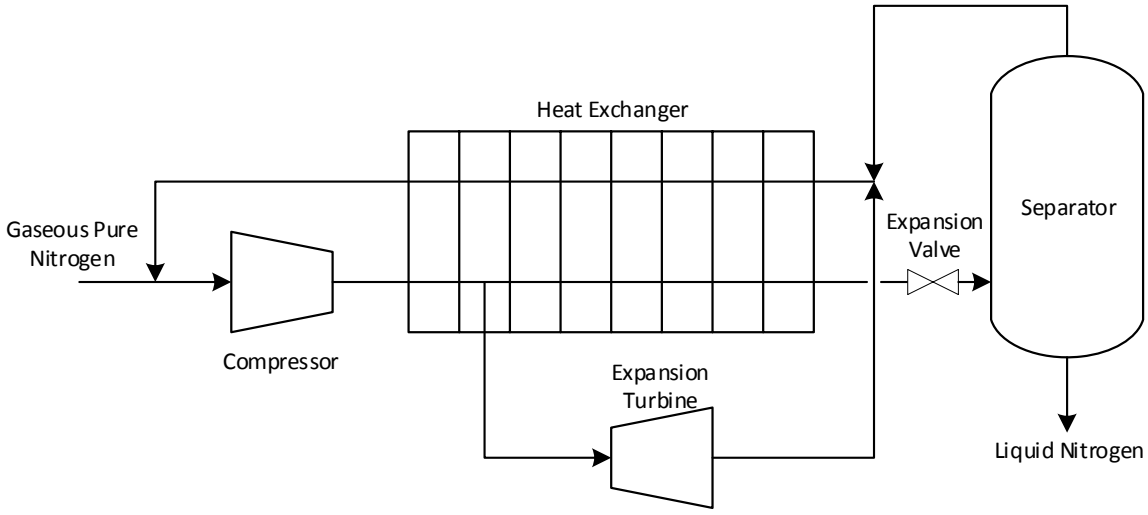

Figure 1: Schematic diagram of the key components of a nitrogen liquefier unit.

External process plants provide advantages of flexibility as they can be run in a batch pattern during off-peak power pricing times without having to support a continuous gaseous tonnage supply network. BOC Gases operate several batch-run NLUs subject to a load management plan (LMP), four of which are considered in this study to provide a range of differing plant loadings for optimisation case studies. Electricity use can be assumed charged on variable half-hourly spot market price tariffs, exposing the power consumption of the power-intensive NLUs to live market price variations. When in operation, NLUs are run at maximum efficiency and subject to an abortive start-up cost that constitutes the energy demand during a transitional start-up mode, whereby electricity consumption is required before liquid nitrogen (LN) production begins. Therefore, the cost of LN production, and ultimately company operational margins, are primarily a function of the optimality of scheduling subject to the expected (and actual outturn) of electricity pricing.

1.2 Current production scheduling policy

Figure 2 provides an overview of the business and production scheduling process. Strategic and tactical business and production planning is completed by running a national distribution optimiser to output a seasonal plan. This is subsequently followed by production scheduling using a bulk liquid optimiser to allocate tankers and drivers, production to site locations and product to customers. Distribution is managed by a delivery planning centre to produce a driver resource, liquid production and customer allocation plan which minimises overall site power, driver manning and fuel costs. This work is carried out by optimisers using established, trusted and proprietary software packages which are not considered to be adjustable by this work. However, the detailed production scheduler layer below is intraday/week scheduling of liquefier and campaign run plant running hours against the UK spot power market and an area of increasing interest due to recent volatility in energy prices.

Detailed production scheduling involves the daily update of the week-ahead NLU LMP for each site using projected customer liquid demands, deliveries and anticipated spot market pricing variation. Renewable generation is a known influence on spot market pricing, however, the impacts are hard to quantify intuitively meaning decisions are made using scheduler instinct and best-guess after observing weather forecasts. The optimiser tools developed in this study are designed specifically to enhance the decision-making process at this level.

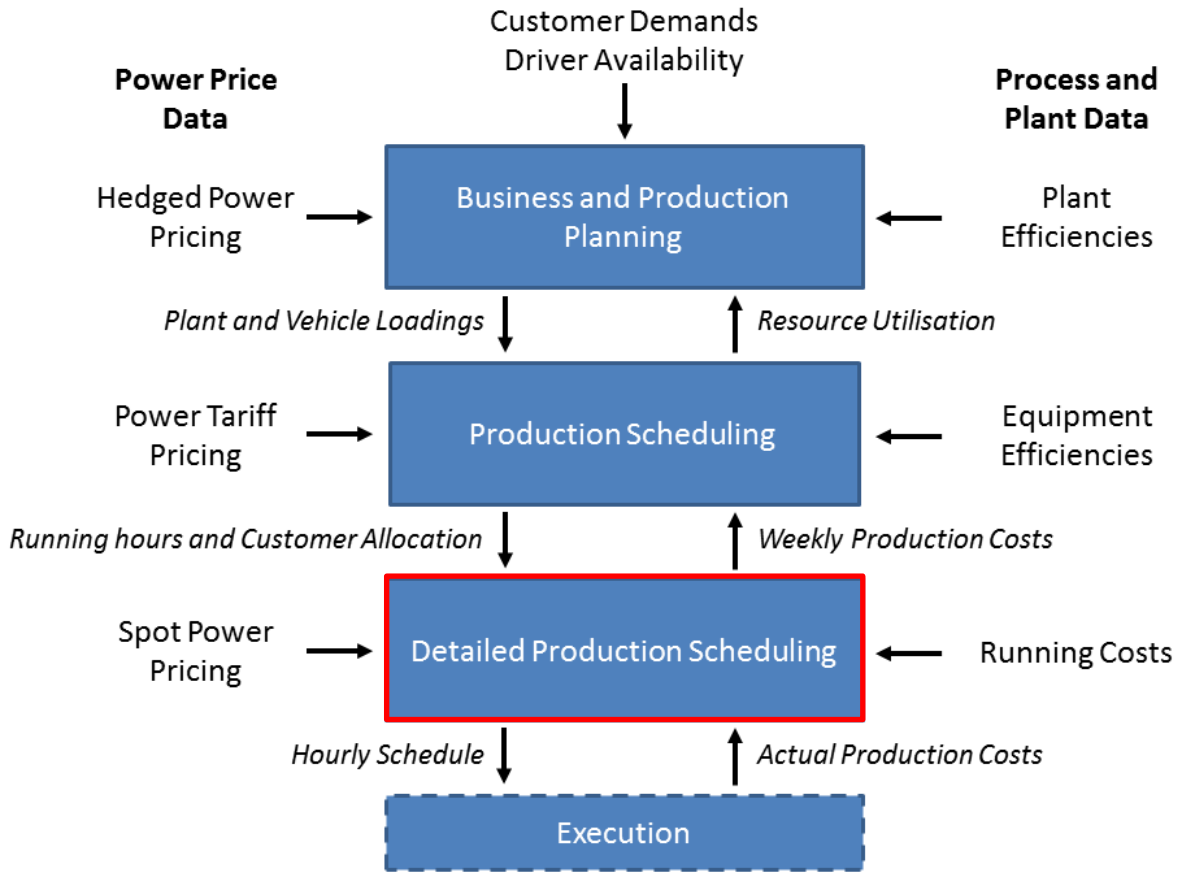

Figure 2: Overview of current liquid production scheduling activities showing all tiers of distribution and production network scheduling and planning. Business planning involves combining forecast customer demands with plant efficiencies to hedge power, production scheduling involves higher detail planning leading to detailed production scheduling (highlighted in red and the focus of this work) which updates the production plan using up to date power pricing and customer demand data.

2.0 Optimal scheduling cost function modelling

A retrospective optimiser (RO) is designed to compare actual operation and the optimal hindsight schedule to generate a missed-potential DSM KPI for each weekly NLU LMP. The results are studied to analyse the scheduling decision making process and improve it for future operational cost reductions. To implement the RO, a mathematical representation of NLU operation may be constructed which consists of three components; (a) the operating cost of the NLU, (b) a description of the abortive start-up costs and (c) consideration of the higher production scheduling level by inter-site optimisation.

The optimiser objective function, J_{NW} (£), minimises the combined NLU network wide (NW) operating cost (assumed a function of electricity price only) of all NLUs considered, N_{NLU}. J_{NW} is the sum of the operating cost of all NLUs over the specified time horizon (one week), given by the spot price of power in each half hour period, $C_{MW,t}$ (£/MWh), and the power demand of the NLU in the same period, $P_{j,t}$ (MWh) summed over the production horizon, N_t,

$$J_{NW} = \sum_{t=1}^{N_t} \left(C_{MW,t} \cdot \left(\sum_{j=1}^{N_{NLU}} P_{j,t} \,.\, w_{j,t} \right) \right) \tag{1}$$

The binary variables, $w_{j,t} \in \{0, 1\}$ ($\forall\, j = 1, \dots, N_{NLU}$ and $t = 1, \dots, N_t$) reflect NLU operation where on (and running at full power) is signalled by a value of '1', and off is given by '0'. The binary coefficients act by removing the cost contribution of NLUs when not in operation.

The overall cost function is constrained by the requirement that each NLU meets the minimum weekly scheduled production running hours – extracted from actual operational data with no uncertainty. Therefore, the actual NLU operational data is defined using a binary variable, $w_{j,t}^{A} \in \{0, 1\}$, reflecting periods when the NLU was either 'on' or 'off'. This allows constraints to be specified, whereby over the production time horizon ($t = 1, \dots, N_t$) the cumulative periods of optimal LN production for each NLU must be greater than or equal to the cumulative periods of actual LN production. This constraint must be individually satisfied for each of the NLUs as follows,

$$\sum_{t=1}^{N_t} w_{j,t}^{A} \leq \sum_{t=1}^{N_t} w_{j,t} \;\forall\, j = 1, \dots, N_{NLU} \tag{2}$$

2.1 Start-up penalties

To identify if an abortive start-up penalty is needed due to a change in the scheduled operational state, a start-up co-efficient, $z_{j,t}$ (MWh), is defined where the operational status of an NLU, $w_{j,t-1}$, in a previous period is subtracted that of the current period, $w_{j,t}$.

$$z_{j,t} = w_{j,t} - w_{j,t-1} \quad \forall\, j = 1, \dots, N_{NLU}\,, t = 1, \dots, N_t \tag{3}$$

The variable generates values that can be manipulated into abortive start-up costs when the NLU power demand is altered from off to on by the optimiser, $z_{j,t} = 1$ MWh. However, it also

produces an unwanted inverse value for when the NLU operational state changes from on to off, $z_{j,t} = -1$ MWh. Therefore, the following constraint is introduced,

$$z_{j,t} - \delta_{j,t} \leq 0 \quad \forall\, j = 1, \dots, N_{NLU}\,, t = 1, \dots, N_t \tag{4}$$

where $\delta_{j,t} \in \{0, 1\}$ is an additional binary variable used to indicate when start-up has occurred, ensuring wherever $z_{j,t} = 1$ MWh, $\delta_{j,t} = 1$. However, it may be noted that the binary start-up variable may still equal 1 when $z_{j,t} = -1$ MWh. To overcome this, an abortive start-up cost penalty for the week and each NLU, $J_{P,j}$ (£), is defined, and added to the cost function in equation 1 to ensure only abortive start-up costs are included within the model. $J_{P,j}$ is a function of the binary start-up variable, $\delta_{j,t}$, the cost of power in the period before the start-up variable is calculated, $C_{MW,t-1}$ (£/MWh), and the start-up power demand in the period before the calculation of $\delta_{j,t}$, $P_{ab,j,t-1}$ (MWh) and is given by,

$$J_{P,j} = \sum_{t=1}^{N_t} \left(C_{MW,t-1} \cdot P_{ab,j,t-1} \cdot \delta_{j,t} \right) \tag{5}$$

Therefore, the overall cost function to be minimised is given by,

$$J_{NW} = \sum_{t=1}^{N_t} \left(C_{MW,t} \cdot \left(\sum_{j=1}^{N_{NLU}} P_{j,t} \,.\, w_{j,t} \right) + \sum_{j=1}^{N_{NLU}} J_{P,j} \right) \tag{6}$$

By minimising equation 6 subject to the constraints in equations 2 and 4, the optimal binary variable values reflecting NLU operation, $w_{j,t}$ and start-up times and frequency, $\delta_{j,t}$ can be determined.

2.2 Inter-site optimisation

Despite normally being in the remit of the bulk optimiser which manages higher level production scheduling, inter-site optimisation capability is also considered as part of the RO due to the geographical proximity of two of the modelled NLUs. Actual operation shows utilisation of one NLU is much greater than that of the other, exposing its operation to the highest power pricing peaks. Inter-site optimisation allows analysis of the potential benefits of transferring production between sites; reducing running hours at one site and re-allocating power consumption to the other at a lower power pricing cost. To represent differences in NLU production rates and increased tanker delivery times an inter-site penalty charge, I_p (£), is applied for every half-hour production period re-directed from one NLU to the other.

Inter-site optimisation may be considered by adjusting equation 2, the constraint on NLU production, so that it could be satisfied by a combination of the production from the two NLUs in question. Therefore, supposing that NLU 2 and NLU 4 are the NLUs subject of the inter-site optimisation, then the equality constraints in equation 2 are modified to give equation 7, which allows total actual production of NLU 2 to be fulfilled by both NLU 2 and 4,

$$\sum_{t=1}^{N_t} w_{2,t}^{A} \leq \sum_{t=1}^{N_t} \left(w_{2,t} + \left(\sum_{t=1}^{N_t} w_{4,t} - \sum_{t=1}^{N_t} w_{4,t}^{A} \right) \right) \tag{7}$$

Where the constraint allows any over-production of NLU 4 to be used to satisfy production demand of NLU 2, an inter-site penalty charge must be incorporated into the model as,

$$J_{int,4} = I_p \cdot \left(\sum_{t=1}^{N_t} w_{4,t} - \sum_{t=1}^{N_t} w_{4,t}^{A} \right) \tag{8}$$

Therefore, the overall cost function to be minimised is given by the combination of equations 6 and 8,

$$J_{NW} = \sum_{t=1}^{N_t} \left(C_{MW,t} \cdot \left(\sum_{j=1}^{N_{NLU}} P_{j,t} \cdot w_{j,t} \right) + \sum_{j=1}^{N_{NLU}} J_{P,j} \right) + J_{int,4} \tag{9}$$

3.0 Retrospective optimisation

As NLU scheduling and optimisation is to be considered on a weekly basis, with decision variables required for each half hourly pricing and operational period (corresponding to the varying spot electricity price settlement periods), the number of running binary variables for each liquefier is given by $N_t = 336$. The total number of liquefiers considered in this study is given by $N_{NLU} = 4$. The optimisers are executed within a Microsoft Excel spreadsheet operating the OpenSolver add-in, see Mason (2012), using the COIN branch and cut linear solver engine. For more information regarding the solver engine we direct the reader to the OpenSolver website. For all results presented, the power demand of each of the NLUs, $P_{j,t}$ (MWh) is assumed to be 10 MWh; with a start-up power demand $P_{ab,j,t}$ (MWh) of 5 MWh (both assumed constant). For inter-site optimisation, a fixed inter-site penalty charge, I_p is used, considered proprietary by this work. For the RO to output potential savings under improved operation, raw data from BOC Gases is sourced consisting of actual NLU operation schedules and the variable half-hourly spot market electricity prices from Epex Spot (2017). To conduct retrospective analysis on the results, full UK electricity generation and demand data, is taken from public access sources, see Elexon (2017) and Sheffield Solar (2017). National Grid data is consolidated regularly to improve accuracy and solar PV generation predictions are generated by sampling 25,000 PV systems to maximise geographical representativeness.

With constraints met, and the optimal values of all the decision variables ($w_{j,t}^{*}$ and $\delta_{j,t}^{*}$) obtained, the NW potential percentage savings, NW_{sav} (%), can be calculated using the actual NW cost, J^{A}(£), and the optimised NW cost, J_{NW} (£). J^{A} is determined by minimising equation 6 with respect to actual NLU operation and the overall potential savings are given by,

$$NW_{sav} = \left(\frac{J^{A} - J_{NW}}{J^{A}} \right) \cdot 100\ \% \tag{10}$$

Equation 10 generates a NW potential cost saving for each NLU which can be used to gain insight into the effectiveness of scheduler decision making after analysis. To conduct detailed analysis of scheduling performance, an 'optimiser score' (OS) is defined to highlight periods of discrepancy between actual and optimal process operation using,

$$\beta_t = \sum_{j=1}^{N_{NLU}} P_{j,t}(w_{j,t}^{A} - w_{j,t}^{*}) \quad (11)$$

Using equation 11, scores range from -40 MWh to 40 MWh where, for example, β_t = -40 MWh corresponds to all 4 NLUs being turned off when the RO suggests they should have all been on and β_t = 40 MWh suggests 4 NLUs were on when they should have been off. Perfect optimal NLU scheduling gives β_t = 0 MWh. OS is determined for all half hourly periods throughout the study and is used as an aid to assess the effectiveness of current scheduling decision making.

3.1 RO results

The RO was used to determine the optimal NLU scheduling operational costs for 13 weeks of actual NLU and power pricing data across late winter and spring 2017. Projected operational cost percentage savings were calculated using equation 10 and shown for each week in Figure 3. Figure 4 shows a histogram frequency plot of the potential hindsight savings of each NLU across the 13-week modelling period, as well as the overall savings, with the average operational cost reduction being 5.82%.

Figure 4 highlights the variation in possible savings for each NLU, with the highest average percentage savings likely for NLU 4 (8.36%) and NLU 1 (8.03%) as these had the lowest utilisations. NLU 2, the most utilised, is the most operationally efficient for its given customer demand constraint, with possible savings of only 3.08%, followed by NLU 3 at 6.35%. Figure 3 illustrates that potential savings range from as little as 0.99% for NLU 2 in week commencing 30/01/17, to 19.79% for NLU 4 in week commencing 10/04/17. A Gantt chart examining the actual and optimal scheduling during 3 days of these weeks is shown in Figure 5. For NLU 2 (high utilisation), the actual and optimal scheduling profiles are similar, whereas for NLU 4 (low utilisation), there are multiple discrepancies.

Referring to Figure 3, only one week demonstrated that inter-site optimisation is effective at reducing costs for the production scheduling level. In week commencing 30/01/17, the RO suggested removing load from NLU 2 and adding it to NLU 4, a change of 1 operational hour. In doing so, the potential savings on NLU 2 increased from 0.99% to 1.96%, savings on NLU 4 decreased from 3.14% to -0.02% and the overall savings increasing marginally from 3.35% to 3.41%. The absence of other results suggests that the production transfer penalty cost used was too great for the inter-site feature to consistently enable worthwhile additional savings.

Further analysis for each week is carried out to determine the maximum I_p value for inter-site optimisation by lowering the value until it is suggested by the optimiser. Figure 6 shows the maximum inter-site penalty cost for inter-site optimisation to take place during each week. It suggests that the reason week commencing 30/01/2017 was highlighted as the inter-site profitable is due to the high NLU 2 loading (97.31%), low loading of NLU 4 (29.85%) and the

high peak pricing seen during late January months caused by cold inclement weather. As NLU 2 utilisation rises, it becomes increasingly difficult to avoid the highest power pricing peaks.

Additionally, Figure 3 shows a deterioration in operational performance with respect to optimal NLU scheduling over the weeks modelled. In summary, as summer approaches, potential savings calculated become much greater. One reason for this may be that during the winter months the peak pricing is much more distinct and predictable based on the TOU, making it is easier to plan around these peaks from an operator's perspective. However, the results demonstrate that significant opportunities for operational cost reduction have been missed during consecutive spring weeks, and seasonal analysis is therefore required in investigate the causes in greater detail.

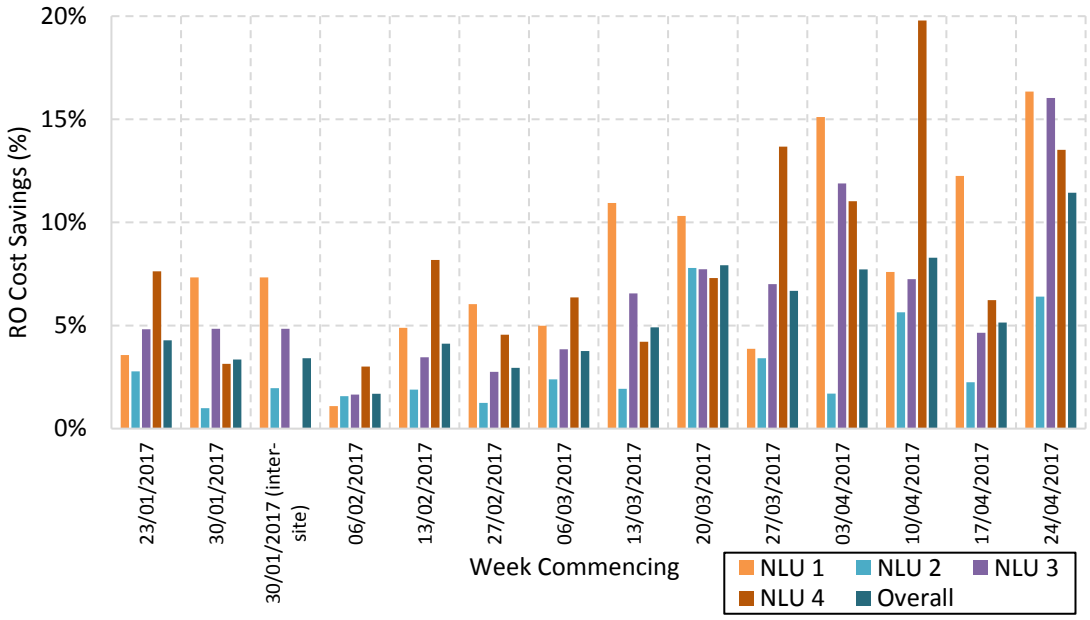

Figure 3: Potential savings estimated by the hindsight RO of all NLUs for each of the weeks optimised.

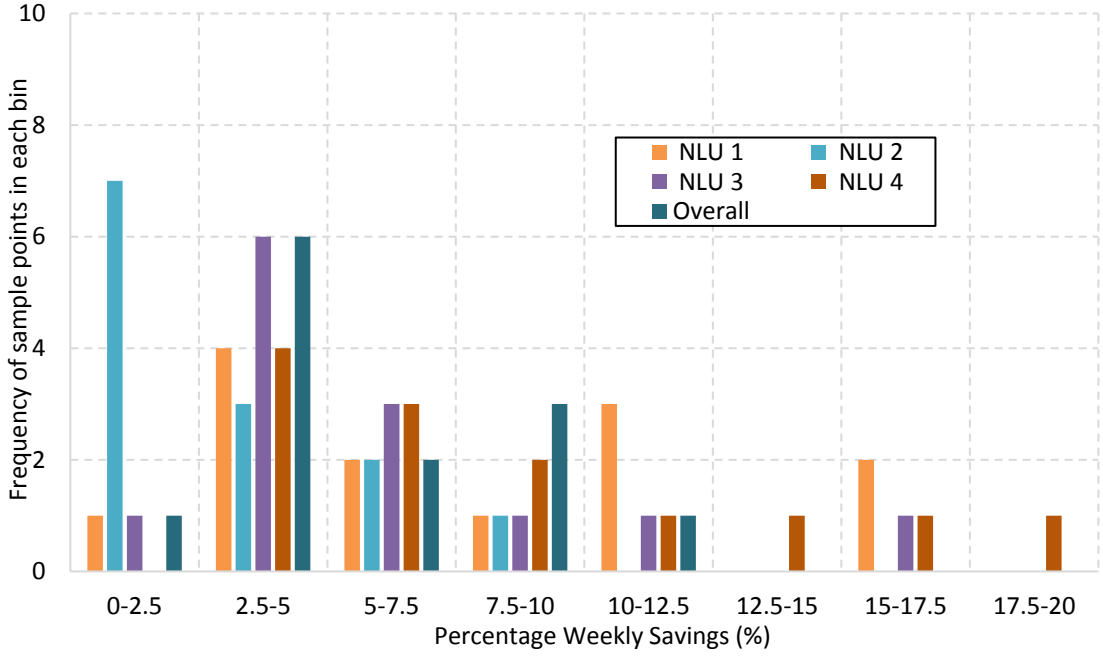

Figure 4: Histogram presenting the frequency of % savings in each bin for each individual NLU and overall.

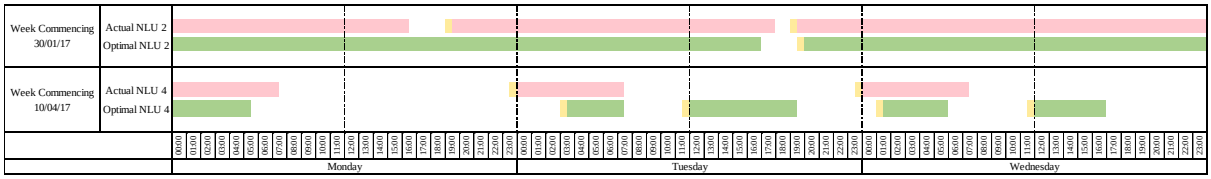

Figure 5: Gantt chart presenting the actual and optimal scheduling of NLU 2 and 4 for 3 days during week commencing 30/04/2017.

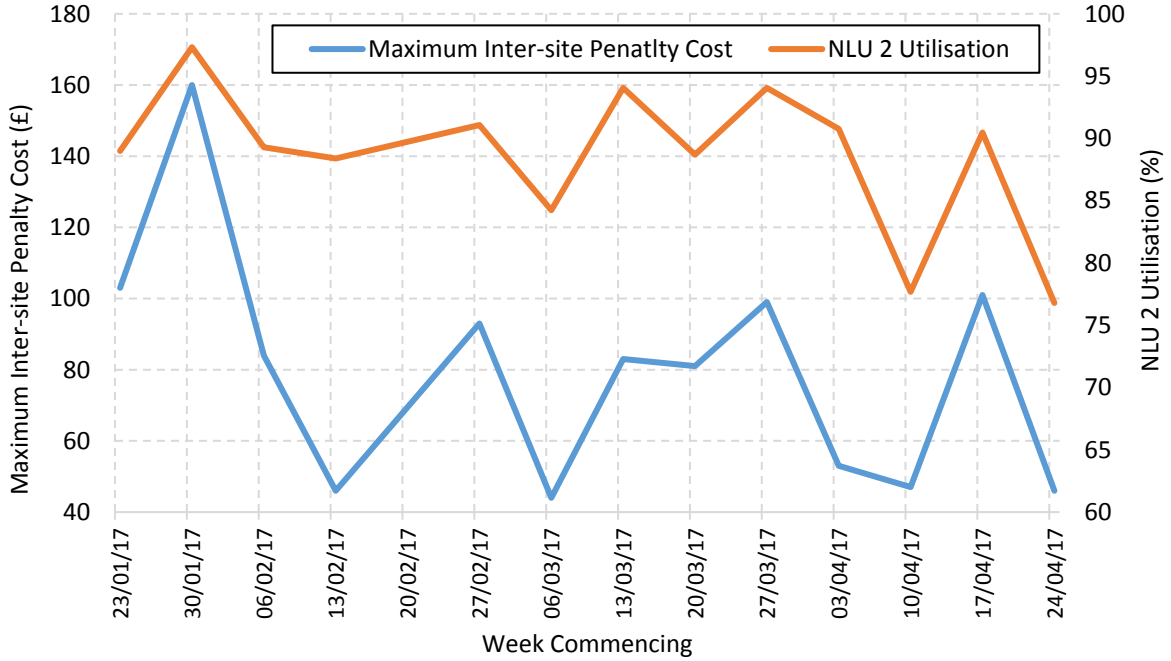

Figure 6: Cost at which inter-site optimisation became viable each week subject to percentage utilisation of NLU 2.

3.2 Seasonal analysis of optimiser score

RO OS analysis is split into late winter (weeks commencing 23/01/17 to 19/02/17) and early spring seasons (weeks commencing 27/02/17 to 30/04/17) to enable the seasonal effects on the results to be isolated. This allows a reduction of the increasing influence of solar generation over the sample period, and the apparent deterioration in scheduling performance, to be excluded from analysis of the results.

Late winter

Figure 7 plots the average OS, defined as an average of the OS's calculated using equation 11, for each daily half hour spot power price period during the 4 winter weeks. Hence, enabling identification of the time periods where optimal and non-optimal scheduling have occurred. Figure 7 can be used as a tool by schedulers to identify and address specific times where scheduling performance has the greatest room for improvement. Figure 7 shows that scheduling performance is typically close to optimal ($\mu\beta_t$ = 0 MWh) for most of the day apart from a tendency to over-consume power ($\mu\beta_t$ = +MWh) during the morning peak (06:30 to 08:00) and under consume power ($\mu\beta_t$ = -MWh) in the late evening (21:00 to 23:00). At the highest points of both peaks the average optimiser score ranges from -10 MWh to +10 MWh. The pattern is representative of the current winter operational strategy; where evening peaks are avoided and day time hours up to peak are utilised to generate additional liquid product. In addition, NLUs are often scheduled to start at 23:00 as standard without checking if earlier start

times would deliver a low marginal cost of operation. The results of this analysis give schedulers reason to re-consider TOU strategies; whilst encouraging a new strategy where NLU operation is increased in the late evening and reduced during the morning peak.

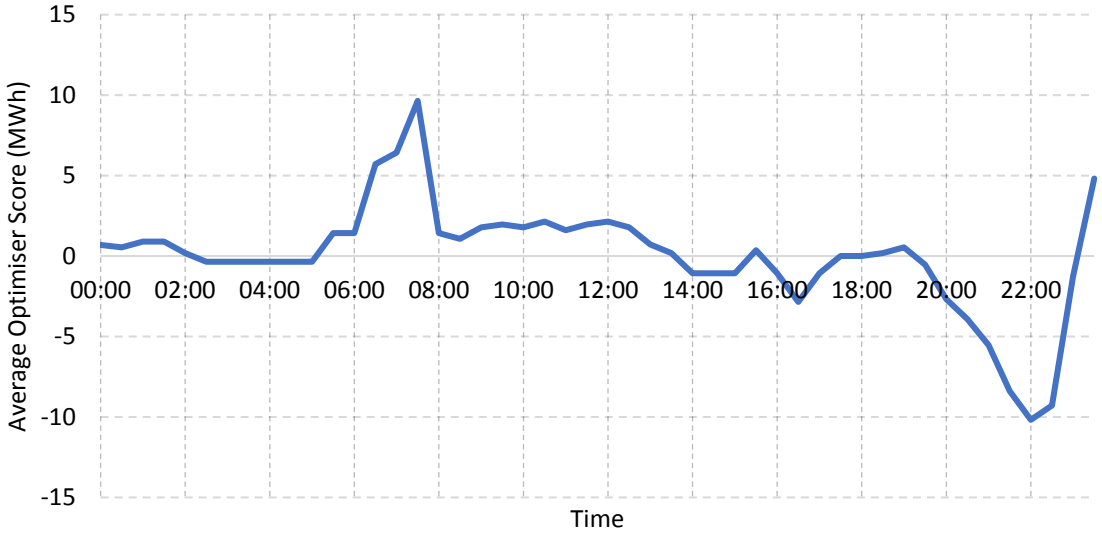

Figure 7: Average optimiser score generated by the RO for each half-hourly period across the winter weeks.

In addition to TOU affects discussed, scheduling operators are aware that increased renewable generation can reduce power prices. The following analysis will inform operators whether they are overly conservative or not conservative enough when altering scheduling strategies based on weather forecasts. Figure 8 specifically considers the impact wind generation has on the RO OS in more detail. It may be observed that there is a linear correlation between the wind penetration percentage and the OS. The average wind penetration is calculated as a percentage of total generation at each value of OS obtained over the 4 weeks; ranging from -30 MWh to +30 MWh (no periods produced scores of ±40 MWh). Figure 8 correlates high wind penetration to missed NLU scheduling opportunities, during which it can be inferred power prices are low. When $\mu\beta_t$ = -30 MWh (3 additional NLUs should have run) the average wind penetration is 13.03%, which proportionally decreases to 6.74% when $\mu\beta_t$ = +30 MWh (turn 3 NLUs off).

Figure 8 shows the frequency at which each of the OS's occurred with NLU operation being optimal most of the time and normally distributed, with smaller numbers of data points referring to the more extreme scores of ±30 MWh. These results confirm the existing operator awareness of wind generation's impact on power pricing, however, on rarer occasions when scheduling is non-optimal, a direct correlation to wind generation can still be drawn, indicating marginally over conservative decision making. Figure 8 can be used to advocate an increased consideration to wind generation when scheduling decisions are made in winter. Due to low solar generation during daytime hours, it is not considered for analysis during the winter months.

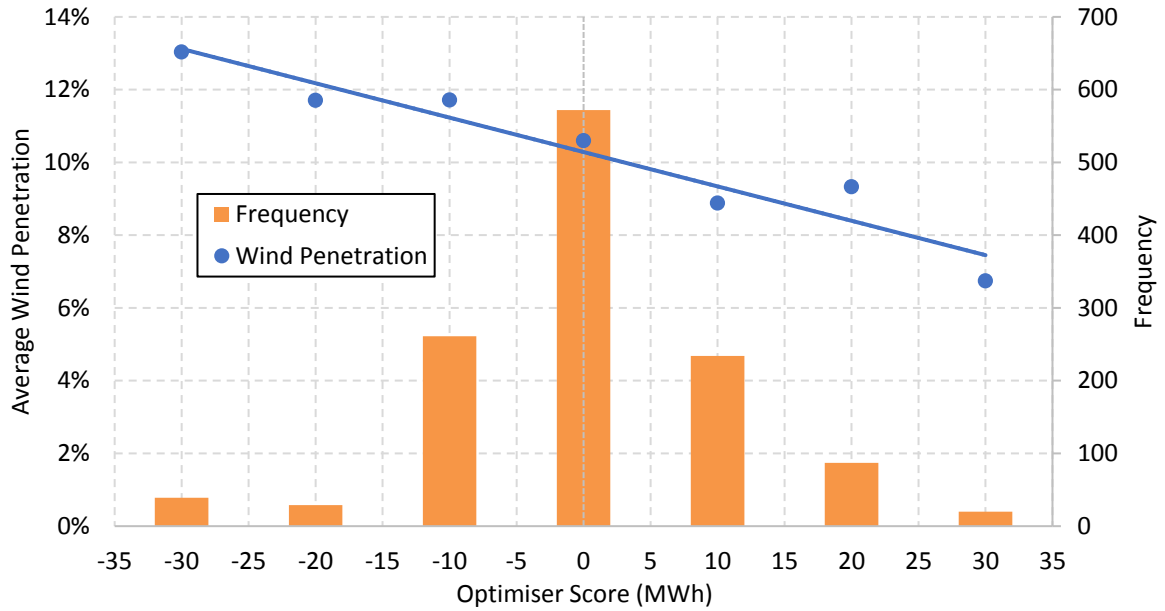

Figure 8: Linear correlation between Optimiser Score and average wind penetration in winter weeks, alongside the frequency at which each optimiser score has occurred.

Early spring

Analysis was repeated for designated spring weeks, where solar generation constitutes a much greater proportion of UK daytime power generation. Similarly to Figure 7, Figure 9 considers the average OS over the day, however Figure 9 concerns itself with the 9 spring weeks of the study. When compared to Figure 7, a similar peak is seen during the morning peak reaching an OS of $\mu\beta_t = 12$ MWh, however the late evening negative peak is now absent. An almost consistent positive OS over $\mu\beta_t = 5$ MWh is visible suggesting over consumption of power overnight during the spring. This power could be re-allocated to periods in the afternoon up to the later evening peak, which display a $\mu\beta_t$ of -10 MWh.

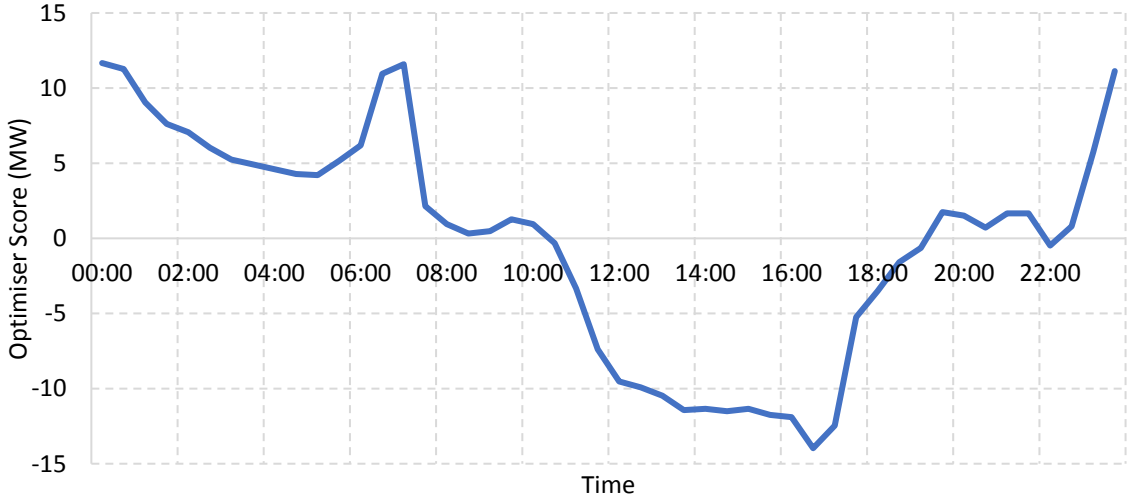

Figure 9: Average optimiser score generated by the RO for each half-hourly period across the spring weeks.

Negative scores in Figure 9 indicate that increasing solar penetration may be lowering afternoon prices, leading to optimal scheduling opportunities being missed as NLU schedulers continue to plan power consumption overnight. Figure 10 considers the impact solar generation had on the RO OS in spring week daytimes (08:00 to 17:30). Figure 10 shows high solar penetrations result in optimiser scores of -30 MW and -20 MW, dropping to around 7% generation at OS of 0 MWh and 10 MWh. Contrasting Figures 8 and 10, a clear difference is visible with regards to the OS distribution. As opposed to the normal distribution in Figure 8 (confirming effective scheduling with a high frequency of 0 MWh optimiser scores), Figure 10 describes a flatter profile. The flat profile indicates that in the spring week daytime hours, non-optimal scheduling decisions are more frequently during low and high solar generation, indicating substantially over conservative decision making. Figure 10 can be used to advocate a significantly increased consideration to solar generation when scheduling decisions are made in spring.

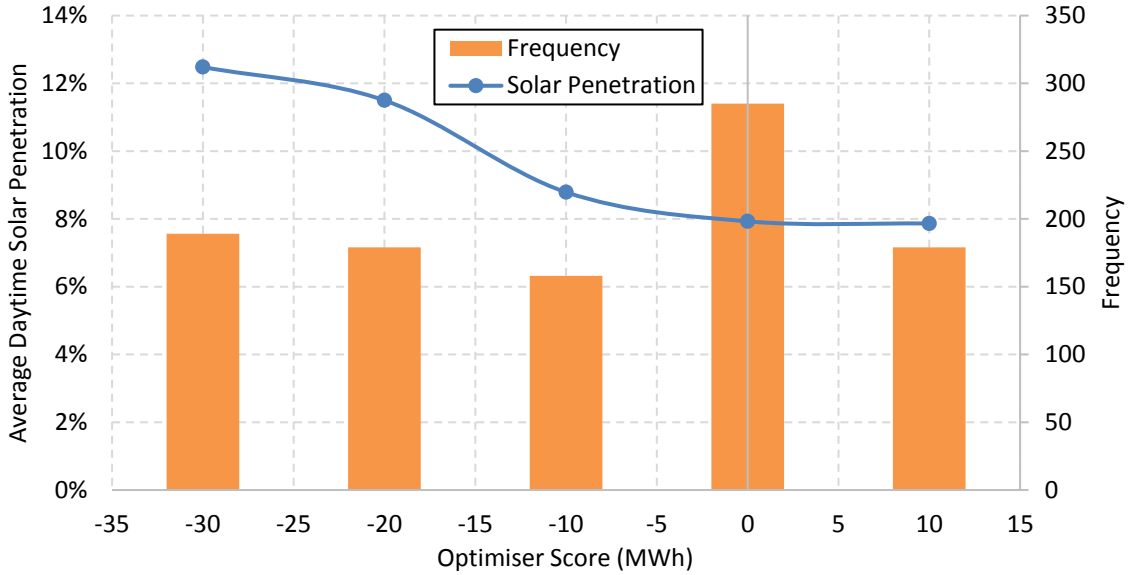

Figure 10: Optimiser Score vs. average daytime solar penetration in spring weeks, alongside the frequency at which each optimiser score has occurred.

The influence of wind penetration during spring weeks has also been assessed, Figure 11 shows a weak correlation, and aside from an outlier at $\mu\beta_t$ = 10 MWh, there is a flat profile when plotting average wind generation percentage against OS. The frequency histogram in Figure 11 is like Figure 8, where a perfect scheduling score of 0 MWh constitutes most of the data points with the remaining normally distributed.

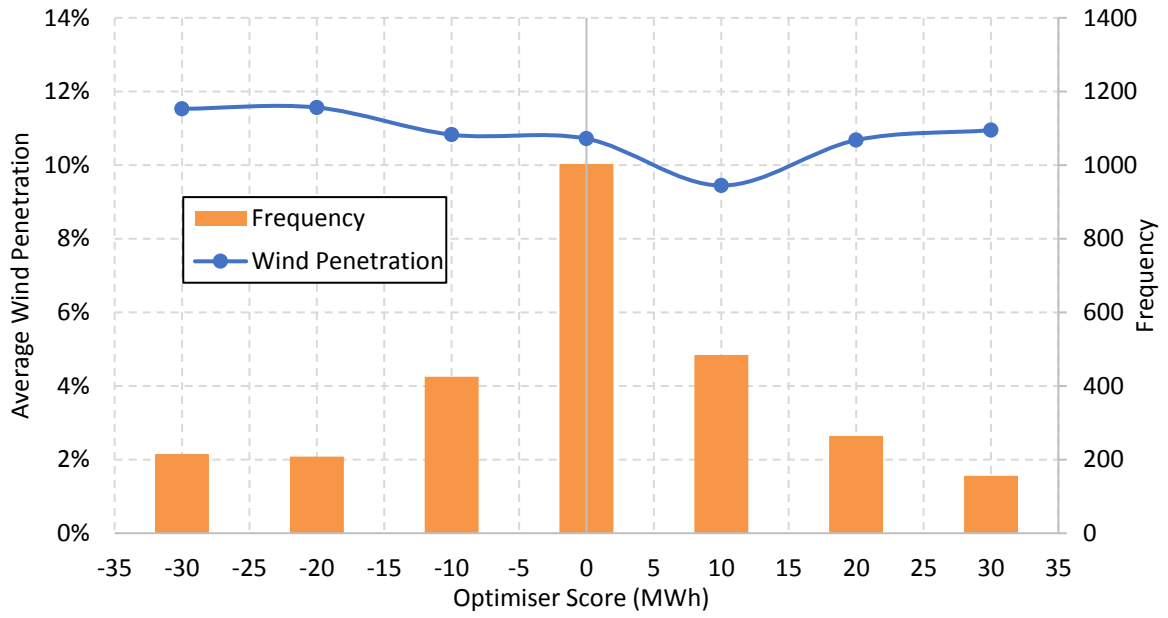

Figure 11: Optimiser Score vs. average wind penetration in spring weeks, alongside the frequency at which each optimiser score has occurred.

Figure 12 plots the effect of combined wind and solar generation on OS for any given half hour throughout a 24-hour period. The correlation graph shows that above a combined intermittent renewable penetration of 20%, the OS indicates that low power price scheduling opportunities are missed. This level of generation can only be achieved during daytime hours when solar is contributing, or during extremely windy conditions. Figures 10 and 12 provide schedulers with a clear reference point that should be used to alter typical operation patterns, whilst suggesting that solar generation is the predominant factor contributing to non-optimal NLU scheduling in the spring months.

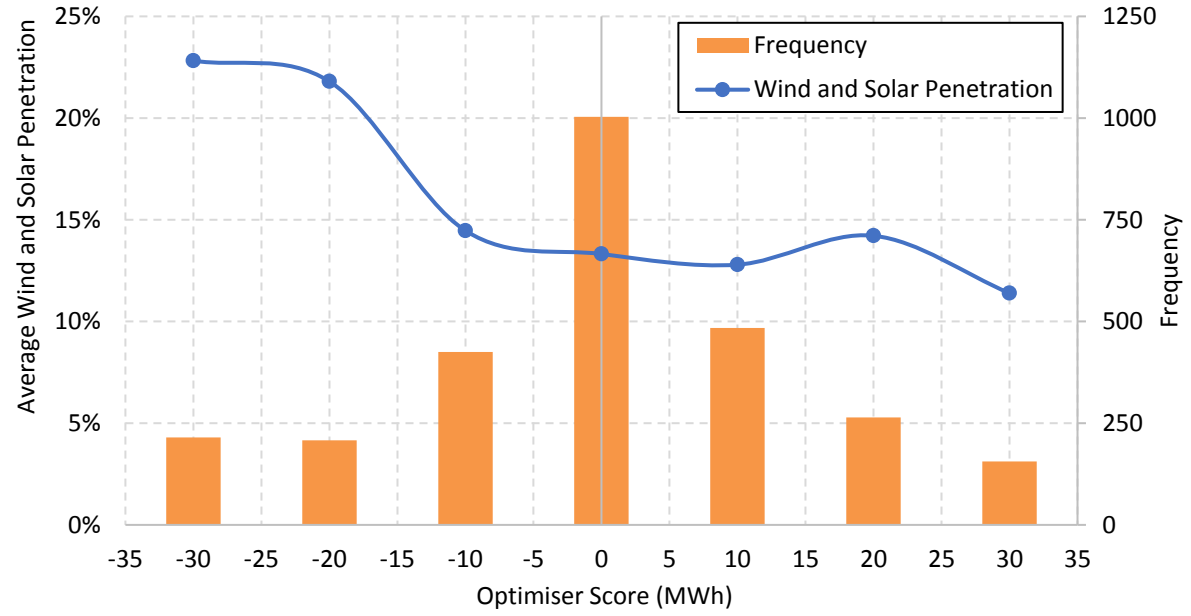

Figure 12: Optimiser Score vs. average (all hours) wind and solar penetration in spring weeks, alongside the frequency at which each optimiser score has occurred.

4.0 Predictive optimisation

A further aim of this work was to develop a tool which automatically generates an optimal schedule of future NLU operation by converting the RO to a predictive optimiser (PO) using forecasts of customer bulk demands and spot market power pricing. Where the renewable generation forecasts for days ahead are known (albeit with some uncertainty), renewable generation and time of power consumption forecasts can be used to generate a pricing forecast. Alongside the learning gained from RO, where thresholds of renewable generation have been identified above which spot power price is reduced and optimal scheduling opportunities are missed, forecasts can be used to optimally schedule the NLU LMP ahead of the TOU.

4.1 Renewable generation influence on power price

Analysis of the results from the RO suggests renewable energy generation, specifically solar and wind penetration, affects the optimality of a given NLU LMP, due to their influence on the spot power price. To review the monetary impact of renewable generation, statistical analysis has been conducted to compare renewable generation percentage, the time of power use and the spot market power price. It is well understood that power price variability comes from many slow and fast-moving factors, such as the system demand and external market conditions such as the price of natural gas respectively. For example, total system demand varies subject to time of day and week, weather (e.g. temperature, cloud cover) and season. Removing this intra-day variability from a produced model will allow a more comprehensive assessment regarding the impact renewable generation sources have on spot power price. To achieve this, generation and spot price data was separated into each half hour period of the day (48 periods) for each of the 7 days of the week. An average power price (μC_{MW}), percentage wind generation (μG_{wind}), percentage solar generation (μG_{solar}) and percentage combined wind and solar generation ($\mu G_{wind+solar}$) is calculated using all sample periods across the 13 weeks at a given half-hourly time. The calculated half-hourly averages can be used to calculate a percentage difference between those values and the actual price at each of all time periods during the 13 weeks of data collected, effectively a difference in generation and price to the average for any given half-hourly period.

Percentage differences in power price compared to the average in each period, from -30% to +30%, are plotted against the average renewable generation percentage difference, when compared to average generation percentage. The range of ±30% power price was selected to encompass most of the time periods studied, excluding any further extreme and less-common price variations from skewing the data due to unexpected grid disturbances, such as loss of a major power generator. Figures 13, 14 and 15 correlate increases or decreases in renewable generation to the spot power price. Figure 13, describing the wind generation to power price correlation, shows a coefficient of determination (R^2) after linear regression of 84%, Figure 14, describing the solar daytime generation and power price correlation has an R^2 of 90%, and Figure 15, showing the linear relationship between combined solar and wind generation and power price over all hours has an R^2 value of 92%.

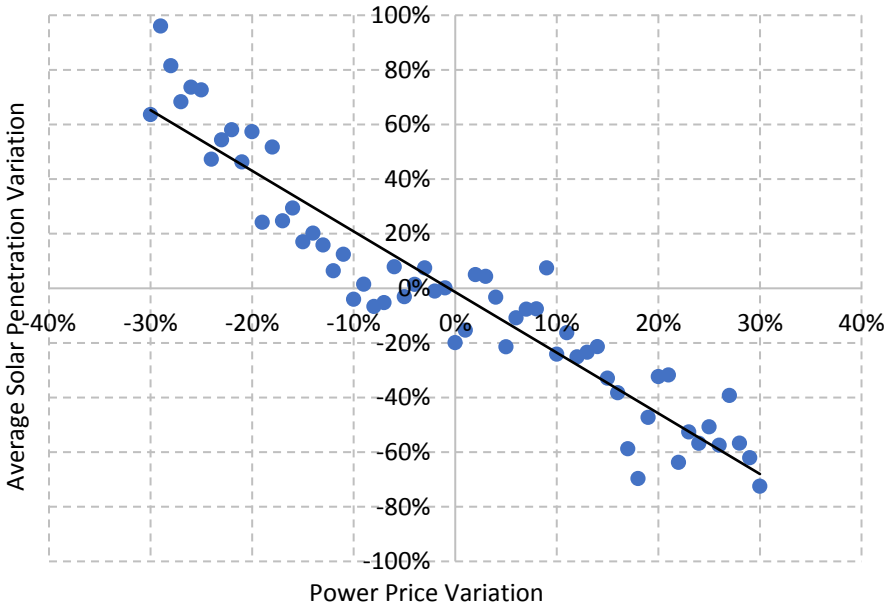

Figure 13: Linear correlation between variation in solar penetration and spot market power price, with the equation of the line given by equation 12.

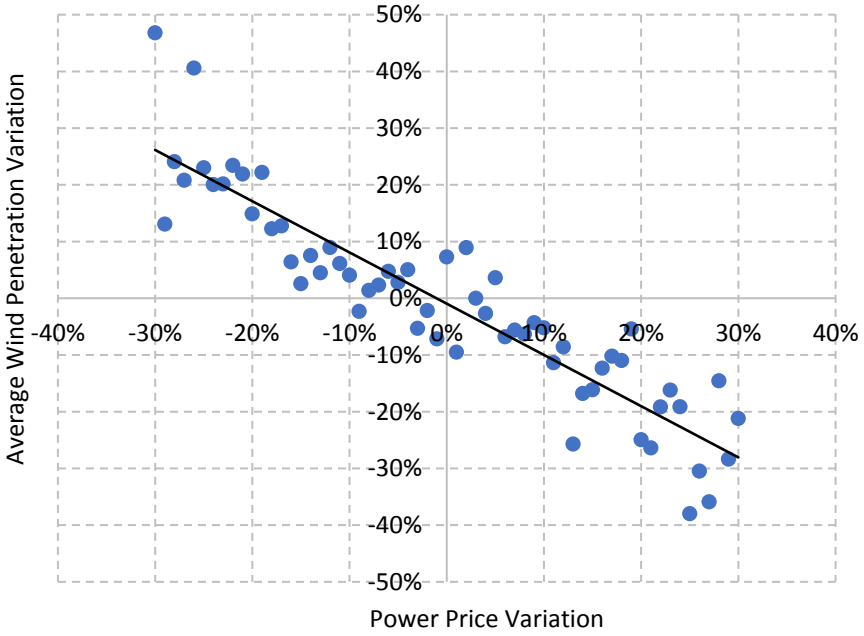

Figure 14: Linear correlation between variation in wind penetration and spot market power price, with the equation of the line given by equation 13.

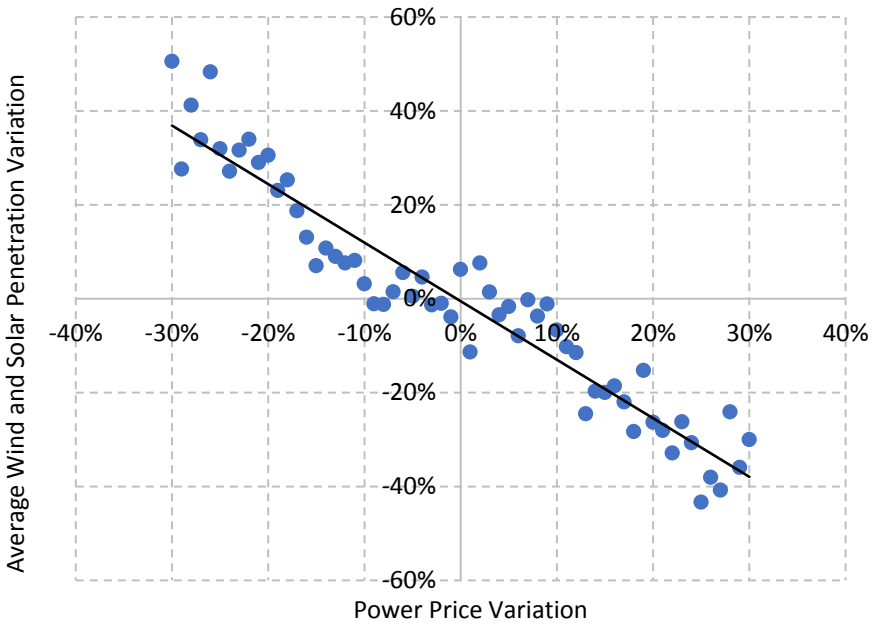

Figure 15: Linear correlation between variation in combined wind and solar penetration and spot power price, with the equation of the line given by equation 14.

All figures show clear trends; where wind or solar generation is increased above the average of all the data points for that half-hourly point in the week, the power price is decreased below the average proportionally. Likewise, when wind and solar generation is limited, the power price tends to rise above its observed average. The correlations shown in Figures 13, 14 and 15 provide schedulers with a quantification tool that can be used to predict power price. Utilising the linear regression equations, the effect of renewables on pricing can be estimated numerically. For example, using all the figures, where solar generation is 84% higher than average, wind generation is 27% higher and the combined wind and solar generation penetration is 37.5% higher, power price can be expected to decrease by around 30% compared to average for that half-hourly period. The linear regression equations for each correlation is given below, where $\Delta\hat{C}_{MW,t}$ (%), is the power price variation from average in each half-hourly period and $\Delta\hat{G}_{ren,t}$ (%) is the renewable generation variation from the total data set average,

$$\Delta\hat{G}_{wind,t} = (-0.9036 \cdot \Delta\hat{C}_{MW,t} - 0.0096) \cdot 100\% \quad (12)$$

$$\Delta\hat{G}_{solar,t} = (-2.2207 \cdot \Delta\hat{C}_{MW,t} - 0.0138) \cdot 100\% \quad (13)$$

$$\Delta\hat{G}_{wind+solar,t} = \left(-1.2472 \cdot \Delta\hat{C}_{MW,t} - 0.0053\right) \cdot 100\% \quad (14)$$

$\Delta\hat{C}_{MW,t}$ is calculated using the power price in each period, $C_{MW,t}$ (£), and the average power price in each period, $\mu C_{MW,t}$ (£).

$$\Delta\hat{C}_{MW,t} = \left(\frac{C_{MW,t} - \mu C_{MW,t}}{\mu C_{MW,t}}\right) \cdot 100\% \quad (15)$$

Similarly, $\Delta G_{ren,t}$, is calculated using the specified renewable generation in each period, $G_{ren,t}$ (£), and the average specified renewable generation, $\mu G_{ren,t}$ (£).

$$\Delta\hat{G}_{ren,t} = \left(\frac{G_{ren,t} - \mu G_{ren,t}}{\mu G_{ren,t}}\right) \cdot 100\% \qquad (16)$$

Using retrospective generation data sourced from Elexon (2017) and Sheffield Solar (2017), $\Delta\hat{G}_{ren,t}$ can be calculated using equation 16; enabling equations 12, 13 and 14 to be re-arranged to calculate $\Delta\hat{C}_{MW,t}$. Finally, equation 15 is also re-arranged in terms of $\hat{C}_{MW,t}$ to predict power price. Limiting constraints are applied to the re-arranged equations 12, 13 and 14, $\Delta\hat{C}_{MW,t}$, due to the range of data utilised,

$$If: \Delta\hat{C}_{MW,t} > 130\%, \qquad \Delta\hat{C}_{MW,t} = 130\%$$

$$If: \Delta\hat{C}_{MW,t} < 70\%, \qquad \Delta\hat{C}_{MW,t} = 70\% \qquad (17)$$

Figures 16 and 17 plot the predicted power prices and the actual power prices for the weeks commencing 13/03/2017 and 24/04/2017. In both Figures, there are clear differences between actual and predicted power prices, with average percentage errors of 20.23% and 17.61% for the weeks commencing 13/03/2017 and 24/04/2017 respectively. Whilst errors occur what is most important is the following of price trends which is particularly visible in Figure 17. During this week, the PO tracks all the major trends qualitatively and therefore gives a strong representation of actual spot power prices, from which very effective scheduling can be derived.

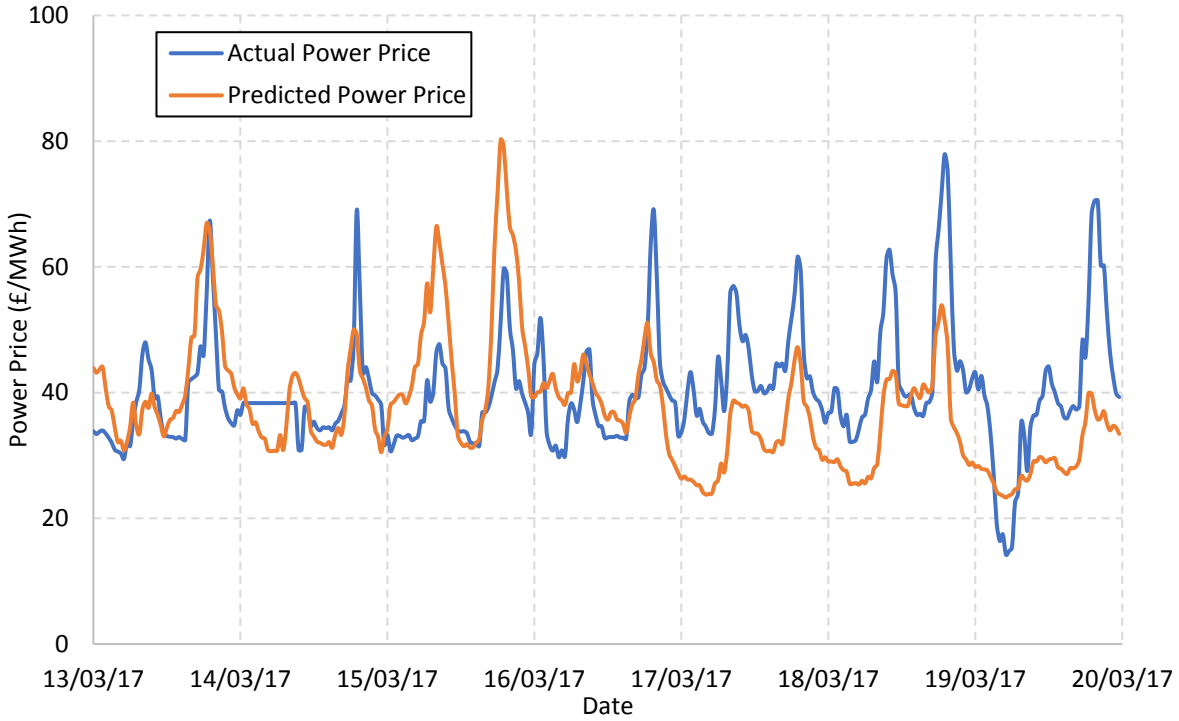

Figure 16: Forecast spot market power price versus actual power price for week commencing 13/03/17.

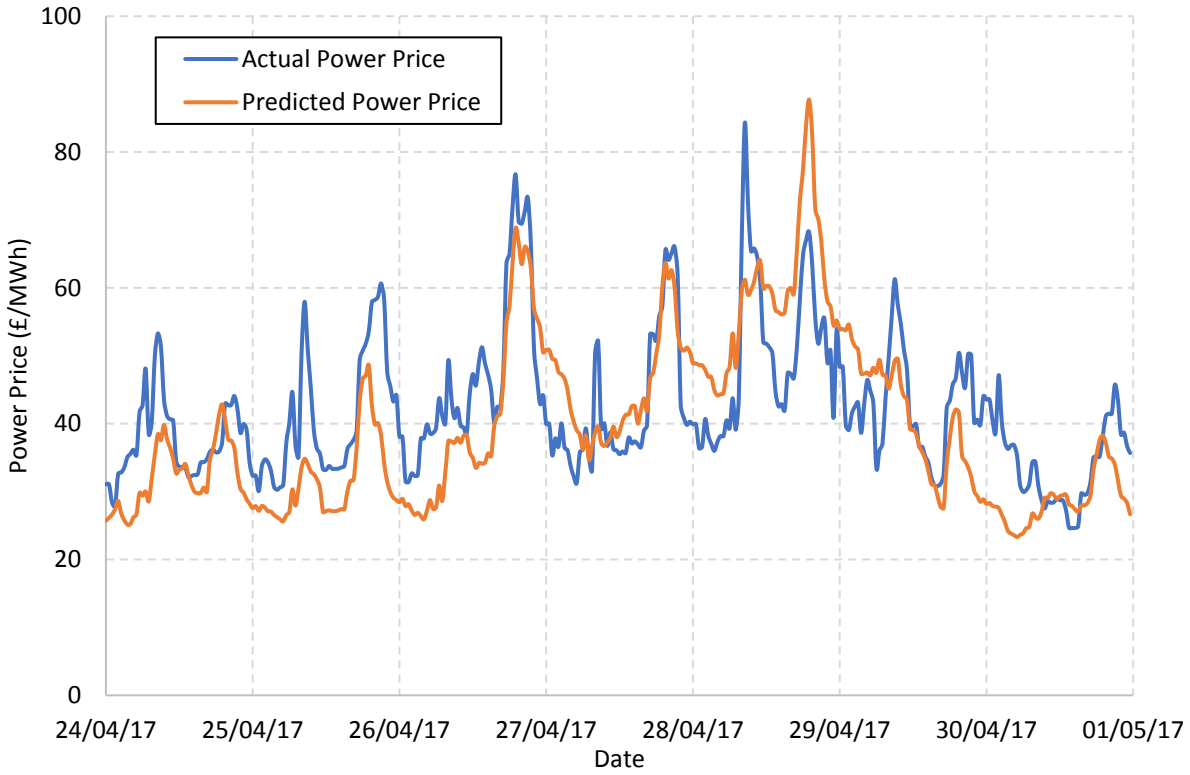

Figure 17: Forecast spot market power price versus actual power price for week commencing 24/04/17.

4.2 PO results

The power pricing forecast is used by the RO rather than the actual power price, along with forecast customer demands at each NLU site, creating a PO whose results can be examined to aid scheduling decision making. As the correlations, see Figures 13, 14 and 15, only represent ±30% price differences, the possible price difference in the PO price forecast is also limited by equation 17 to ±30% to ensure power pricing is predicted only within the modelled space.

Figure 18 shows the potential savings for the PO during the winter weeks using both the wind to spot power price correlation, and the combined wind and solar to power price correlation, whilst Figure 19 describes the PO savings profiles for the spring weeks using just the combined wind and solar spot power price correlation.

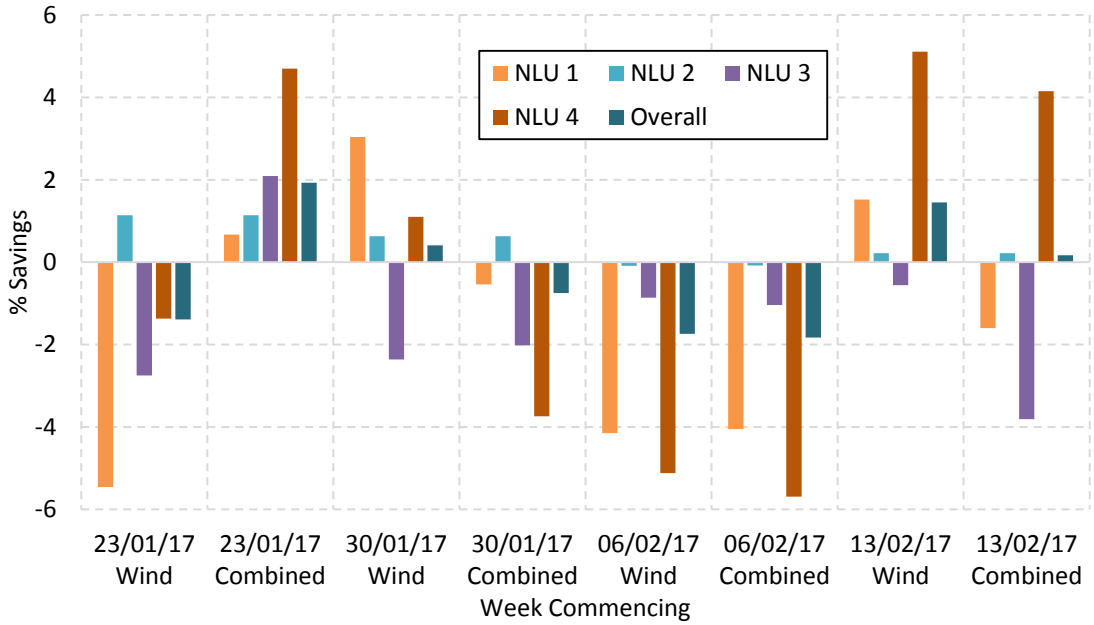

Figure 18: Potential savings available for each NLU individually and overall using either the combined or wind generation pricing correlation for PO scheduling in winter weeks.

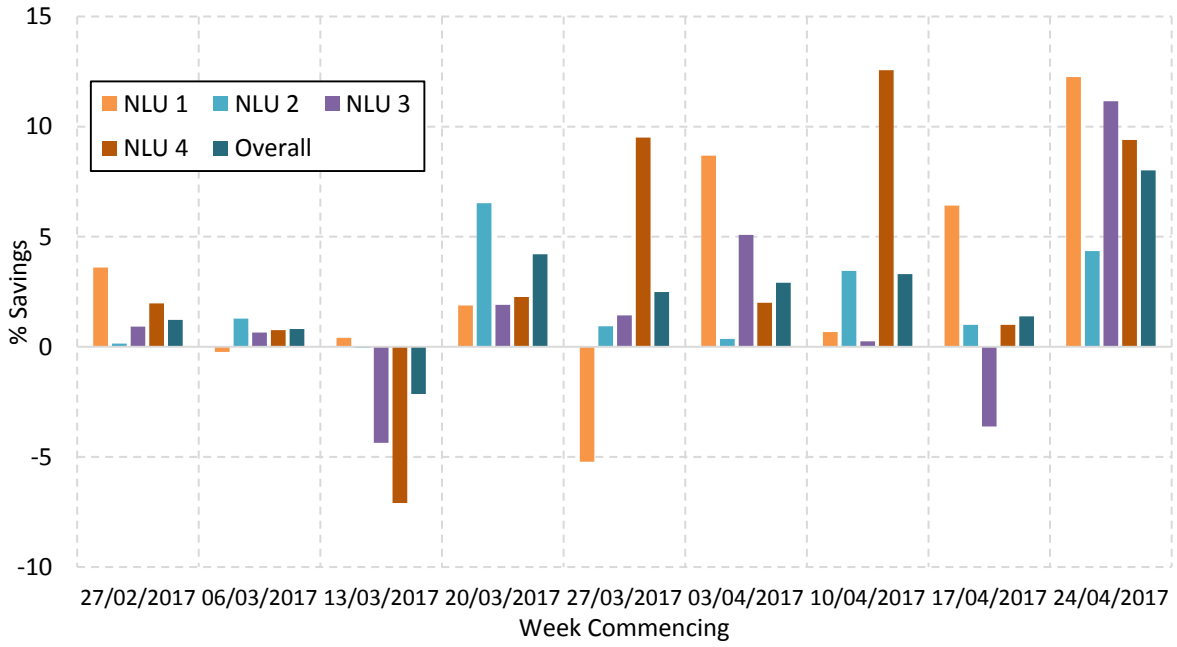

Figure 19: Potential savings available for each NLU individually and overall using the combined wind and solar generation pricing correlation for PO scheduling in spring weeks.

Figure 18 shows that during winter weeks the PO does not project sustainable additional savings. Using the wind correlations only, the overall result is an additional loss of 0.31% compared to actual operation, whilst the combined correlation provides an additional loss of 0.12%. These small losses suggest that to capitalise on the savings possible from the RO, schedulers would be best directed editing the operation patterns using Figure 7 rather than implementing the PO. The losses indicate that during winter weeks the TOU has a larger impact on power prices rather than high renewable generation, nevertheless schedulers should remain opportunistic under high wind generation as encouraged by Figure 8. A potentially limiting

factor of the PO in winter weeks is only allowing ±30 % difference compared to average period power price, this is not truly representative of winter spot power pricing when peaks have been seen to rise 200% above average prices under certain external market trading conditions. Further development work could improve the PO during winter periods but even the RO demonstrated smaller savings compared to summer periods.

During the spring weeks, the performance and effectiveness of the PO is much stronger. Using the combined correlation to predict power prices, and then using the power price forecast in the PO to produce an optimal schedule produced an average saving over the 9 weeks of 2.5%. Figure 19 repeats the pattern displayed in Figure 3 with potential savings rising with increasing potential solar generation capacity. Aside from the week commencing 13/03/2017, operational costs are reduced in every spring week when implementing the PO using a power pricing forecast based on generation data. Losses seen in this week can be explained as an outlier due to the erratic late week/weekend power prices that the PO, limited to ±30% price variation, struggled to predict, see Figure 16. The highest saving achieved is 8.01% during the week commencing 24/04/2017, where the PO price predictor displayed strong power price trend tracking, see Figure 17, that has facilitated effective predictive scheduling performance. The PO has shown it can generate increasing savings as spring moves towards summer; if implemented during the summer months, schedulers could significantly reduce operational costs by reacting to the growing impact of solar generation on spot market power pricing.

5.0 Discussion and conclusions

In this paper, a RO has been designed and implemented to show the potential operating energy cost savings available after optimal scheduling of four NLUs at varying utilisations. The optimisation model includes an integrated NLU abortive start-up cost penalty, and an inter-site optimisation capability which can redirect customer demand to alternative sites in the interest of cost savings. The abortive start-up cost penalty replicates actual operational start up, whilst preventing numerous unrealistic NLU stops which would increase operator workload and cause excessive machine wear. Retrospective analysis (and optimisation) has identified specific behaviours for where scheduling can be improved, and has driven the development of a PO that uses regression models to predict power prices using renewable energy generation data, enabling specification of future NLU production schedules in advance. This makes the model much more broadly accessible and implementable for real NLU operation than the previous simulation study work discussed in the literature review. Cost function modelling may be improved further by more accurately describing each NLU's actual power consumption, LN production rate and inter-site penalty cost individually within the optimiser.

Ultimately, the RO provides BOC Gases with a weekly hindsight NLU scheduling KPI benchmark, whilst generating data that can be retrospectively analysed to enhance optimal scheduling practise. To provide schedulers with a week-ahead optimal schedule of NLU LMPs, predictive pricing models that correlate wind and solar generation to their impact on power price have been developed with variability caused by the day of the week and time of the day removed from the data. Strong linear correlations are observed in the ranges of ±30% variance from average power price and the average wind, solar or combined generation. For time periods

where power price dropped 30% below average, the solar, wind and combined generations averaged 84%, 27% and 37.5% above their average generation contributions respectively.

The linear correlations formed the basis of the PO, where actual renewable generation data was used to predict spot market power pricing. It was shown that the power price predictions may be used to develop alternative schedules which could then be compared to actual NLU scheduling for economic assessment of scheduler performance. During winter weeks, using both wind and combined wind and solar power price prediction correlations, the PO generated small loses of 0.35% and 0.13% respectively when compared to actual operation. The PO model showed limited effectiveness during this period inhibited by the maximum allowable ±30% price variation that does not truly reflect winter price volatility. However, applied to spring weeks the combined wind and solar correlation PO model averaged savings of 2.52%, which cumulates to significant monetary value in the energy intensive LN production process. The results also demonstrated larger savings were possible as the date progressed to summer due to increasing solar generation which contributes to lower daytime power prices. The highest overall PO saving was found in the final week of the study at 8%.

Future work will enable the PO to use future National Grid generation predictions to estimate power prices using the correlation model, whilst also considering ways to expand model robustness beyond ±30% price variation. The models can be periodically updated, similarly to ARIMA based models, to detect changes in renewable generation performance and external market conditions. The ever-increasing potential savings results shown by both the RO and PO are only likely to increase as solar penetration becomes greater over the summer period, it is therefore probable that application of the PO will generate substantial future operating cost savings. The PO can be used at the start of the week and at the daily scheduling meeting as National Grid predictions are updated. The results can be compared to actual operation, and if savings are still suggested by the PO, it can be deployed as an implementable scheduling tool. Even with schedules set by the PO, operators would be advised to stay responsive to extremely high periods of renewable penetration (over 22%); using the correlations between these circumstances and high negative optimiser scores (-30 MWh), to justify more flexible and confident scheduling decisions. Over time, it is expected that the RO DSM KPIs will reduce, indicating better optimal load scheduling of NLUs. This work is envisaged to be relevant for retrospective and predictive scheduling of other energy intensive industrial batch processes, and perhaps optimal scheduling charging and discharging of energy storage technologies.

Acknowledgments

The authors gratefully acknowledge the financial support of EPSRC grant EP/G037620/1 and BOC Gases through the Biopharmaceutical Bioprocessing Technology Centre and School of Chemical Engineering and Advanced Materials at Newcastle University, UK.

References

Adamson, R., Hobbs, M., Silcock, A. and Willis, M. (2017a) “Steady-state optimisation of a multiple cryogenic air separation unit and compressor plant” Applied Energy 189 221-232.

Adamson, R., Hobbs, M., Silcock, A. and Willis, M. (2017b) “Integrated real-time production scheduling of a multiple cryogenic air separation unit and compressor plant” Computers and Chemical Engineering 104 25-37

Bentzen, J. and Engsted, T. (2001) “A revival of the autoregressive distributed lag model in estimating energy demand relationships” Energy 26(1) 45-55.

Boogert, A. and D. Dupont (2008) “When supply meets demand: the case of hourly spot electricity prices” IEEE Transactions on Power Systems 23(2) 389-398.

Croos-Dabrera, R., Wunderink, R., Rello, J., Cammarata, S. and Kollef, M. (2004) “Clinical cure and survival in Gram-positive ventilator-associated pneumonia: retrospective analysis of two double-blind studies comparing linezolid with vancomycin” Intensive Care Medicine 30(3) 388-394.

Daryanian, B., Bohn, R. and Tabors, R. (1989) “Optimal demand-side response to electricity spot prices for storage-type customers” IEEE Transactions on Power Systems 4(3) 897-903

Dambier, M. and Hinkelbein, J. (2006) “Analysis of 2004 German general aviation aircraft accidents according to the HFACS model” Air Medical Journal 25(6) 265-269

Duzgun, R. and Thiele, A. (2010) “Robust Optimization with Multiple Ranges: Theory and Application to R & D Project Selection” (submitted to European journal operational research)

Elexon (2017) “Balancing Mechanism Reporting Service: Electricity Data Summary” data from https://www.bmreports.com/bmrs/?q=eds/main [accessed 15 May 2017]

Epex Spot (2017) “EPEX SPOT Power UK Spot Dashboard” data from https://www.apxgroup.com/market-results/apx-power-uk/dashboard/ [accessed 15 May 2017]

Floudas, C. A., Lin, X. (2005). “Mixed integer linear programming in process scheduling: modelling, algorithms, and applications” Annals of Operations Research 139 131-162

Gupta, V., I. E. Grossmann, S. Pathak and J. André (2012) “Assessing the benefits of production-distribution coordination in an industrial gases supply chain” CMU repository

Guthrie, G. and S. Videbeck (2007) “Electricity spot price dynamics: Beyond financial models” Energy Policy 35(11) 5614-5621

Hall, L. M. H., A. R. Buckley and J. Mawyin (2015) “Estimating the Impact of Wind Generation in the UK” (submitted to Journal of Energy Policy)

Hamid, M. F. A. and Shabri, A. (2017) “Palm oil price forecasting model: An autoregressive distributed lag (ARDL) approach” AIP Conference Proceedings 1842(030026)

Ierapetritou, M., Wu, D., Vin, J., Sweeney, P. and Chigirinskiy, M. (2002) “Cost Minimization in an Energy-Intensive Plant Using Mathematical Programming Approaches” Industrial & Engineering Chemistry Research 41(21) 5262-5277

Kargar, Z. S., Khanna, S., & Sattar, A. (2013) “Using prediction to improve elective surgery scheduling” The Australasian Medical Journal 6(5) 287–289

Karwan, M. and Keblis, M. (2007) “Operations planning with real time pricing of a primary input” Computers & Operations Research 34(3) 848-867

Karakatsani, N. and Bunn, D. (2004) “Modelling the Volatility of Spot Electricity Prices” Available at: http://www.agsm.edu.au/bobm/iows/bunn_volatility_04c.pdf [accessed 21 May 2017]

Lewis, N., Collins, D., Pedlar, C. and Rogers, J. (2015) “Can clinicians and scientists explain and prevent unexplained underperformance syndrome in elite athletes: an interdisciplinary perspective and 2016 update” BMJ Open Sport & Exercise Medicine 1(1) e000063

Manenti, F. and Rovaglio, M. (2013) “Market-driven operational optimization of industrial gas supply chains” Computers & Chemical Engineering 56 128-141

Marchetti, P. A., V. Gupta, I. E. Grossmann, L. Cook, P.-M. Valton, T. Singh, T. Li and J. André (2014) “Simultaneous production and distribution of industrial gas supply-chains” Computers & Chemical Engineering 69 39-58

Mason, A. (2012) “OpenSolver – An Open Source Add-in to Solve Linear and Integer Progammes in Excel” Operations Research Proceedings [online]301-406. Available at: http://opensolver.org/ [Accessed 21 May 2017]

Merkert, L., Harjunkoski, I., Isaksson, A., Säynevirta, S., Saarela, A. and Sand, G. (2015). “Scheduling and energy – Industrial challenges and opportunities” Computers & Chemical Engineering 72 183-198

Mitra, S., Grossmann, I., Pinto, J. and Arora, N. (2012a) “Optimal production planning under time-sensitive electricity prices for continuous power-intensive processes” Computers & Chemical Engineering 38 171-184

Mitra S, Grossmann IE, Pinto JM, Arora N (2012b) “Robust scheduling under time-sensitive electricity prices for continuous power-intensive processes” Proceedings of the Foundations of Computer-Aided Process Operations 2012

National Grid (2016) “Summer Outlook Report 2016” 30-57 Available at: http://www2.nationalgrid.com/WorkArea/DownloadAsset.aspx?id=8589934747 [accessed 04/09/2017]

Ofgem (2015) “Wholesale Energy Markets in 2015” 53–54 Available at: https://www.ofgem.gov.uk/sites/default/files/docs/2015/09/wholesale_energy_markets_in_2015_final_0.pdf [accessed 15 May 2017]

Sheffield Solar (2017) "Live PV generation" from https://www.solar.sheffield.ac.uk/pvlive/ [accessed 15 May 2017]

Swinand, G. and Godel, M. (2012) “Estimating the impact of wind generation on balancing costs in the GB electricity markets” 4th Workshop on Energy and CO2 Markets, Valencia

Syed, M. (2016) “Black Box Thinking: The Surprising Truth About Success” published by Hachette UK

Weron, R. Misiorek, A. (2005) “Forecasting spot electricity prices with time series models” Proceedings of the European Electricity Market EEM-05 Conference, Lodz, 133–141

You, F., J. M. Pinto, E. Capón, I. E. Grossmann, N. Arora and L. Megan (2011a) “Optimal distribution-inventory planning of industrial gases. I. Fast computational strategies for large-scale problems” Industrial & Engineering Chemistry Research 50(5) 2910-2927

You, F., J. M. Pinto, I. E. Grossmann and L. Megan (2011b) “Optimal distribution-inventory planning of industrial gases. II. MINLP models and algorithms for stochastic cases” Industrial & Engineering Chemistry Research 50(5) 2928-2945

Zareipour, H., Canizares, C. and Bhattacharya, K. (2010) “Economic Impact of Electricity Market Price Forecasting Errors: A Demand-Side Analysis” IEEE Transactions on Power Systems 25(1) 254-262

Zhang, Q., A. Sundaramoorthy, I. E. Grossmann and J. M. Pinto (2016) "A discrete-time scheduling model for continuous power-intensive process networks with various power contracts" Computers & Chemical Engineering 84 382-393

Zhu, Y., Legg, S. and Laird, C. (2011) "Optimal operation of cryogenic air separation systems with demand uncertainty and contractual obligations" Chemical Engineering Science 66(5) 953-963